An Induction Generator-Based AC/DC Hybrid Electric Power Generation System for More Electric Aircraft

Yijiang Jia, *Student Member, IEEE*, and Kaushik Rajashekara, *Fellow, IEEE*

***Abstract*—In more electric aircraft (MEA) system, both ac and dc electric power with multiple voltage levels are required for various aircraft loads. This paper presents an induction generator-based ac/dc hybrid electric power generation system for MEA. In the proposed system architecure, a high-speed induction starter/generator and a low-speed induction generator are installed on the high pressure (HP) and low pressure (LP) spools of the engine, respectively. In generating mode of operation, all of the constant voltage variable frequency ac power is generated by the HP generator while the dc power demand is shared by both HP and LP generators. A control scheme is developed to regulate the ac load voltage and coordinate dc power generation between the two generators. The proposed induction generator based ac/dc hybrid generation system results in reduced hardware requirement compared with both ac and dc primary generation systems.**

***Index Terms*—Aircraft, distributed power generation, genrators, induction motors, power generation control.**

I. Introduction

THE EMERGING trend toward more electric architecture for airplanes is intended to replace mechanical, hydraulic, and pneumatic systems with electrical systems as much as possible. It is generally considered that the more electric aircraft (MEA) would lead to lower fuel consumption and emissions, reduced maintenance, and possibly lower costs [1]–[4]. Advancements of on-board electrification have increased the electric power demand of the aircraft. A significant raise of generation capacity is required to supply the additional loads.

As is shown in Fig. 1, in present MEA systems (e.g., Boeing 787, Airbus A380), the wound-field synchronous generator (SG)-based ac primary generation system [5], [6] can feed the frequency insensitive loads directly from the SG terminals. The constant voltage variable frequency (CVVF) ac load voltage is regulated by controlling the field current of the SG through an external brushless exciter. This exciter consists of a permanent magnet (PM) machine and a diode rectifier mounted on the generator shaft. By adjusting the excitation of the field winding, the ac source voltage can be regulated with variable shaft speed. However, in the SG-based ac primary generation system, the complex rotor structure makes the torque to inertia ratio of SG lower than other type of electric machines [1]. Moreover, the rotating diode bridge structure limits the top speed of the generator shaft. If the synchronous machine is used as a starter/generator, separate field and armature voltage controls are required during its motoring operation.

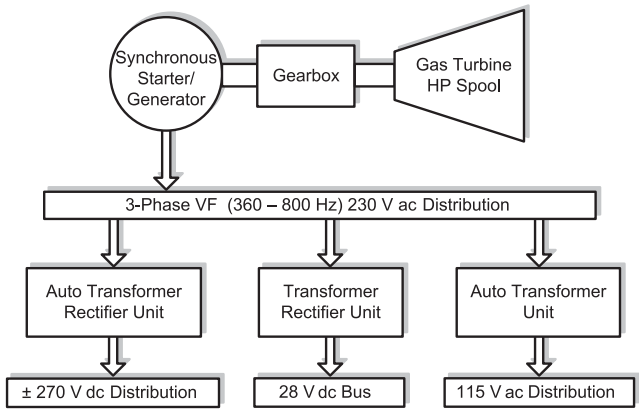

Fig. 1. System configuration of the SG-based ac primary generation system [6].

In MEA systems, the effect of electrical power offtake can sometimes have significant impact on the dynamics and control of the aircraft engine [7]. For instance, during the transition from cruise to descent phase, the aircraft engine power is transiently reduced while maintaining high electrical power demand. This transition creates a possibility of engine instability and may require substantial electric load shedding. This issue can be resolved by installing an extra generator on the low pressure (LP) spool of the engine and sharing the electrical power extraction between the high pressure (HP) and LP spools [4]–[7].

In order to parallel the two generators operated at different frequencies, a dc primary generation system with power electronic converters is preferred as an advanced more electric architecture [8], [9]. PM generator is preferred in this twin-spool twin-generator architecture due to its high-power density and self-excited capability [8]–[10]. As shown in Fig. 2,

Manuscript received August 16, 2016; revised November 20, 2016; accepted December 24, 2016. Date of publication January 10, 2017; date of current version May 18, 2017. Paper 2016-IACC-0892.R1, presented at the 2015 IEEE Industry Applications Society Annual Meeting, Dallas, TX, USA, Oct. 18–22, and approved for publication in the IEEE TRANSACTIONS ON INDUSTRY APPLICATIONS by the Industrial Automation and Control Committee of the IEEE Industry Applications Society.

Y. Jia is with the University of Texas at Dallas, Richardson, TX 75080 USA (e-mail: yxj131230@utdallas.edu).

K. Rajashekara is with the University of Houston, Houston, TX 77004 USA (e-mail: ksraja@uh.edu).

Color versions of one or more of the figures in this paper are available online at http://ieeexplore.ieee.org.

Digital Object Identifier 10.1109/TIA.2017.2650862

0093-9994 © 2017 IEEE. Personal use is permitted, but republication/redistribution requires IEEE permission.
See http://www.ieee.org/publications_standards/publications/rights/index.html for more information.

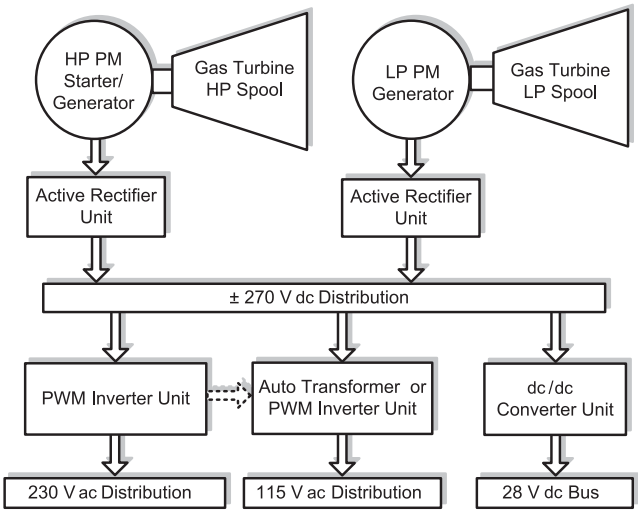

Fig. 2. System configuration of the PM generator-based dc primary generation system [8].

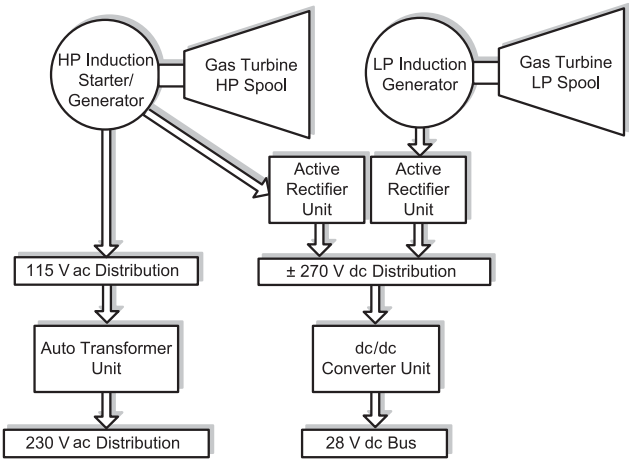

Fig. 3. System configuration of the IG-based ac/dc hybrid generation system.

a high-speed starter/generator and a low-speed generator are placed directly on the HP and LP spool of the engine, respectively. In the engine starting process, the PM starter/generator on HP spool can operate as a motor to start the engine using ground power supply. During the flight mission, the power generated from the two generators are rectified and transmitted to a ±270-V dc power bus. This type of system presents high power factor and high efficiency, but suffers from excessive current flow during fault condition because of the use of PM generators [10]. Although multiphase fault-tolerant PM generators have been investigated to limit the short-circuit fault current [11]–[13], using PM generator to fulfill the overload current requirement of main engine generator in aerospace application is still problematic. Furthermore, installing the PM generator close to the gas turbine engine may greatly affect the system reliability since most PM materials are vulnerable to demagnetization under very high temperature. Finally, compared to the SGbased ac primary generation system architecture, the CVVF power demanded by frequency insensitive loads (e.g., wing de-icing system, galleys, etc.) in dc primary generation system is first converted to dc power by the active rectifier of the generator, and inverted back to ac power through dedicated inverters. This two-stage ac–dc–ac conversion adds extra losses and additional hardware to the system. In Boeing 787, under cursing condition, the power consumed by the frequency insensitive ac loads is close to 50% of the total electrical power consumption [8].

Using induction machine as main engine generator in aircraft application is rarely reported in literature [14]–[16]. In medium power applications (50–150 kW), the power density of induction generator (IG) is relatively higher than wound-field SG, but lower than PM generator [17]. Nonetheless, the concern of excessive fault current due to the PM excitation for airborne applications can be easily addressed by using IGs. In addition, the internal impedance of IG is the lowest among all type of generators.

From the generation system architecture point of view, since neither ac nor dc primary generation system is able to meet all the power requirements with optimized performance in terms of volume, weight, efficiency, reliability, and cost. Hence, in this paper, an IG-based ac/dc hybrid generation system is proposed to combine the advantages and address the shortcomings of both systems.

In this paper, the configuration of the proposed IG-based ac/dc hybrid generation system for MEA is presented. A steady-state analysis is carried out to explain the proposed twin-spool twin-generator ac/dc hybrid generation method. A closed-loop control scheme for ac and dc voltage regulation of the proposed system is developed based on field oriented control (FOC) theory. As an extension of the work in [18], the feasibility of operation of the proposed system is demonstrated by hardware-in-the-loop real-time emulation.

II. System Configuration

The proposed IG-based ac/dc hybrid generation system is shown in Fig. 3. In the proposed system, a high-speed open-end winding squirrel-cage induction starter/generator and a low-speed conventional wye-connected squirrel-cage IG are attached to the HP and LP spools of the engine, respectively. In generating mode of operation, the HP generator is in charge of generating all of the CVVF power, while the dc power demand is shared by both HP and LP generators. The proposed ac/dc hybrid generation architecture can supply CVVF power directly from one side of the generator winding terminals without external exciter, and generate dc power on the other side of the generator winding terminals through an inverter/rectifier unit.

From the generation system architecture point of view, compared to dc primary generation system in Fig. 2, the undesired ac–dc–ac conversion is avoided by applying ac/dc hybrid generation on HP spool in the proposed system, while the merits of the twin-spool twin-generator dc primary generation architecture have been reserved. As compared to the ac primary generation system in Fig. 1, the application of IG removes the external exciter, while the twin-spool twin-generator architecture improves

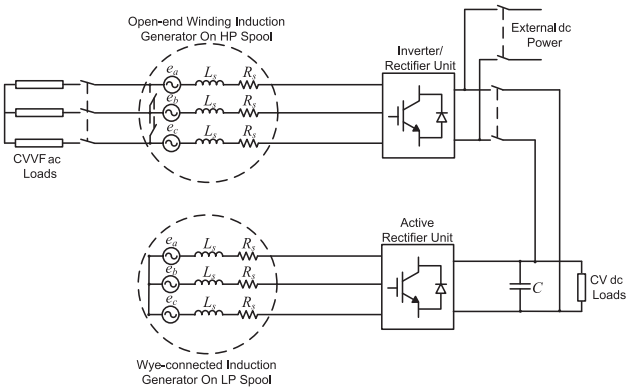

Fig. 4. Electrical system diagram of the IG-based ac/dc hybrid generation system.

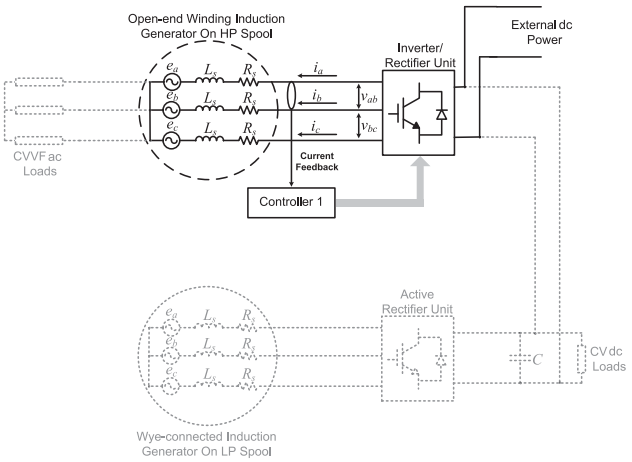

Fig. 5. Starter mode of operation of the IG-based ac/dc hybrid generation system.

the overall generation performance. As a result, the overall hardware requirement of the proposed system is reduced compared to both ac and dc primary generation systems.

A more detailed electrical system configuration is shown in Fig. 4. An inverter/rectifier unit and frequency insensitive ac loads are connected to each end of the HP spool open-end winding IG terminals. An active rectifier unit is connected to the LP spool wye-connected IG. The dc output end of the inverter/rectifier unit and the active rectifier unit are paralleled to the dc bus.

In most of the MEA applications, besides generating electric power, the main engine generator is also used as a starter for starting the aircraft engine. A dc power supply from the APU generation system or ground power supply is usually available for this process. As is shown in Fig. 5, in the engine starting mode of operation, the entire LP spool generation subsystem is deactivated. The ac loads are disconnected from the HP generator, and the ac load-side generator terminals are shorted to transform the open-end IG on HP spool into a wye-connected induction motor. Additional circuit breakers are required to implement this transformation. Using the dc power supply, the transformed

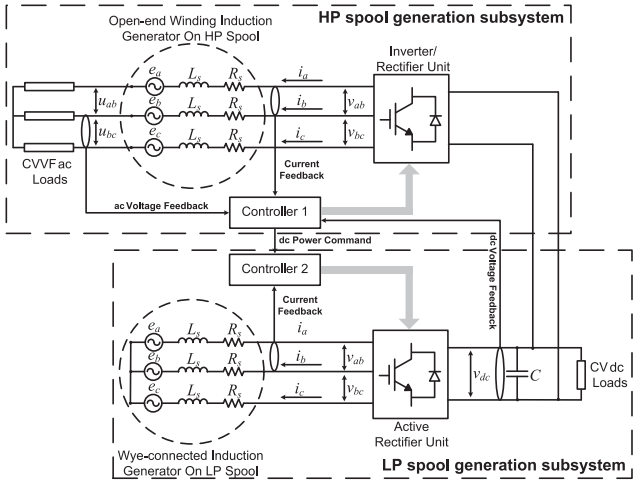

Fig. 6. Generator mode of operation of the IG-based ac/dc hybrid generation system.

induction motor can be driven by the inverter/rectifier unit to start the aircraft engine.

Once the engine shaft reaches its idle speed, the proposed system begins to operate in generator mode. As is shown in Fig. 6, in this mode of operation, the ac load-side terminals of the HP generator are connected to the CVVF loads, and the wye-connected IG on LP spool is activated. All the CVVF power is generated only by the HP generator, while the power demand of the dc loads is shared between both the HP and LP generators. The dc-bus capacitor will be fully charged at the beginning of the generator mode of operation.

In the proposed ac/dc hybrid generation system, instead of using a conventional wye-connected IG and connecting the CVVF loads in parallel with the inverter/rectifier unit [19], the CVVF loads, the HP shaft open-end winding IG, and the inverter/rectifier unit are connected in series. Compared to the conventional shunt connected configuration [19], the series connected inverter/rectifier unit requires higher current ratings. However, the open-end winding generator configuration can increase the output voltage of the generator [20], [21], from which the current rating of the generator can be reduced for the same amount of power generation demand. As a result, the size and weight of the generator can be greatly reduced compared to the shunt connected configuration.

III. System Modeling and Operation Principle

As is shown in Fig. 6, in the proposed generation system, all the CVVF power is only generated by the HP generator, while the power demand of the dc loads is shared between both the HP and LP generators. The generation subsystem on HP spool includes a high-speed generator, an inverter/rectifier unit, a CVVF distribution bus, and a shared CV dc distribution bus. The generation subsystem on LP spool consists of a low-speed generator, an active rectifier unit, and the shared CV dc distribution bus. The system model and operation principle of the generation subsystems on HP and LP spools are discussed in detail in the following sections.

A. HP Spool Generation Subsystem and AC Load Voltage Regulation

In the HP spool generation subsystem, the frequency insensitive loads in MEA (e.g., wing de-icing system and galley loads), which are generally resistive heaters, are symmetrically distributed at the generator terminals. Therefore, the open-end winding IG on HP spool can be modeled as a wye-connected IG with an increased stator resistance. In the rotor flux oriented reference frame, neglecting the saturation effects, the steady-state voltage and torque equations for the HP spool IG can be expressed as [17]

$$V_{qs1} = (R_{s1} + R_{acL})\, I_{qs1} + \omega_{e1}\lambda_{ds1} \tag{1}$$

$$V_{ds1} = (R_{s1} + R_{acL})\, I_{ds1} - \omega_{e1}\lambda_{qs1} \tag{2}$$

$$T_{e1} = \frac{3}{2}\frac{P1}{2}\frac{{L_{m1}}^2}{L_{r1}} I_{qs1} I_{ds1} \tag{3}$$

$$\lambda_{qs1} = L_{s\sigma 1} I_{qs1} \tag{4}$$

$$\lambda_{ds1} = L_{s1} I_{ds1} \tag{5}$$

$$L_{s\sigma 1} = L_{s1} - \frac{L_{m1}^2}{L_{r1}}. \tag{6}$$

In the above equations, V_{qs1}, V_{ds1}, I_{qs1}, I_{ds1}, λ_{qs1}, and λ_{ds1} are the q- and d-axis stator voltages, currents, and flux linkages, respectively. R_{s1} is the stator winding resistance and R_{acL} is the ac load resistance. $L_{s\sigma 1}$ stands for the stator transient inductance (stator short-circuit inductance). L_{s1}, L_{r1}, L_{m1}, and P1, are the stator, rotor, magnetizing inductance, and pole pairs of the induction machine 1, respectively. ω_{e1} is the electrical frequency of the induction machine 1.

In the proposed system, the ac loads (resistive heaters) are modeled as three-phase balanced resistors connecting in series with HP generator windings. In order to regulate the ac RMS load voltage, the ac load current (stator current magnitude) needs to be controlled according to the load resistance variation. The ac line-to-line RMS load voltage can be expressed as

$$v_{ac} = \sqrt{v_{a1}^2 + v_{b1}^2 + v_{c1}^2}. \tag{7}$$

The ac load current reference can be expressed as

$$I^* = \sqrt{{I_{qs1}^*}^2 + {I_{ds1}^*}^2}. \tag{8}$$

Limited by the current rating of the generation system, the power generated for frequency insensitive ac loads can be modeled as the heat generated by the three-phase balanced resistors connected in series with the HP generator. Thus, the power transmitted to the dc bus can be written as

$$P_{dc1} = -\omega_{e1}\frac{T_{e1}^*}{P1} - (R_{s1} + R_{acL})\, I^{*2} \tag{9}$$

where T_{e1}^* is the torque reference of the HP generator.

According to (9), the torque reference can be determined by the ac load current reference and dc power output command. The theoretical equilibrium points of the HP spool generation subsystem for a given ac and dc power demand are illustrated in Fig. 7.

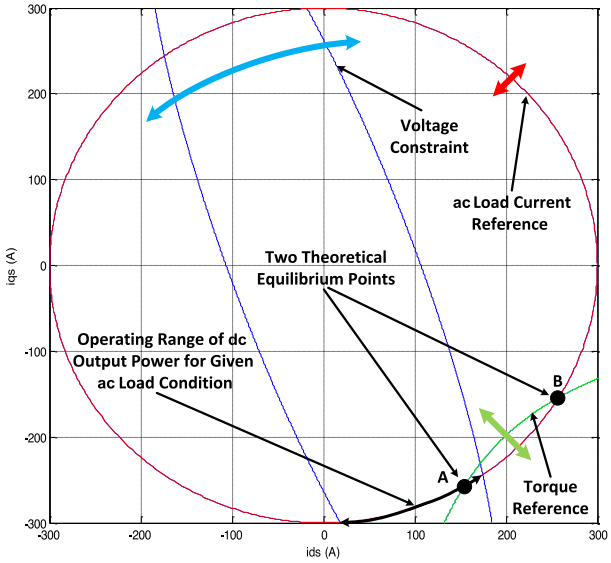

Fig. 7. Operating constraints of the HP spool generation subsystem.

In Fig. 7, the intersections A and B indicate two theoretical equilibrium points for corresponding ac load current and HP generator torque references. For a given ac load condition, the torque reference of the HP generator varies with different dc output power command of the system. When the dc power output increases, the torque reference curve will move away from the ac load current reference circle. Therefore, the dc power output needs to be limited to ensure that there exists at least one intersection point of the torque reference curve and the load current reference circle.

Furthermore, the maximum torque of an IG is limited by the voltage rating of the system. This voltage limitation can be expressed as follows:

$$V_{s1,\max}^2 \geq V_{qs1}^2 + V_{ds1}^2 \tag{10}$$

Substituting (1), (2), (4), (5) into (10), the voltage constraint equation becomes

$$\left[\frac{(R_{s1} + R_{acL})\, I_{qs1}}{\omega_{e1}} + L_s I_{ds1}\right]^2 + \left[\frac{(R_{s1} + R_{acL})\, I_{ds1}}{\omega_{e1}} - L_{s\sigma 1} I_{qs1}\right]^2 \leq \frac{V_{s1,\max}^2}{\omega_{e1}^2}. \tag{11}$$

Equation (11) forms a voltage limit ellipse in Fig. 7. This ellipse is similar to the analysis of flux weakening operation for induction motor [22], yet the load resistance makes the ellipse rotation varies from different load condition in the proposed system. An increased ac load power demand will result in a clockwise rotation of the voltage limit ellipse and vice versa. Therefore, equilibrium point B in Fig. 7 is not a valid operating point of the system. Besides the constraint to guarantee the existence of equilibrium point, the dc output power from HP spool is hereby further bounded by the voltage limit of the

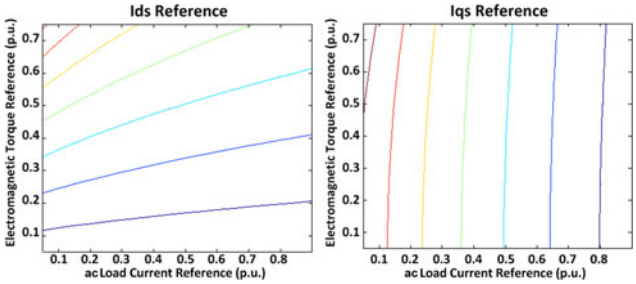

Fig. 8. Contour maps of d-q axis current commands for ac load current and generator torque reference sweep test.

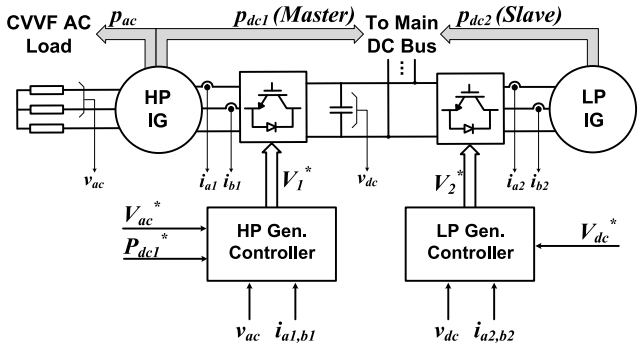

Fig. 9. Overall closed-loop control scheme for the proposed ac/dc hybrid generation system

system. This bounded operating range can be demonstrated as the segment of the ac current reference circle inside of the voltage limit ellipse.

The flux current command I_{ds1}^* and torque current command I_{qs1}^* can be calculated as the simultaneous solution of (3) and (8). For a given ac load current reference and HP generator torque reference, the d and q-axis current references can be expressed as follows:

$$I_{ds1}^* = \frac{\sqrt{I^{*2} - \frac{2T_{e1}^*}{k_1}} - \sqrt{I^{*2} + \frac{2T_{e1}^*}{k_1}}}{2} \tag{12}$$

$$I_{qs1}^* = \frac{-\sqrt{I^{*2} - \frac{2T_{e1}^*}{k_1}} - \sqrt{I^{*2} + \frac{2T_{e1}^*}{k_1}}}{2} \tag{13}$$

where $k_1 = \frac{3}{2}\frac{P1}{2}\frac{L_{m1}^2}{L_{r1}}$ is the torque coefficient.

In order to illustrate the disposition of d-, q-axis current commands with ac and dc power demand variations, a two-dimensional sweep test of ac load current and generator torque reference is performed using MATLAB.

The results of the test are shown as contour maps in Fig. 8. Evidently, the q-axis (torque) current command and ac load current reference variations are almost proportional, while changing q-axis current command has little impact to the generator torque with a fixed ac load current command. The d-axis (flux) current command changes greatly with generator torque variation, but it is relatively insensitive to ac load current changes. It can be inferred from the sweep test results that changing dc power output of the HP spool generation subsystem greatly depends on the flux variation of HP generator, resulting in a very slow system response. In contrast, regulating ac load voltage with a constant (or slowly varied) dc output power can be achieved by controlling q-axis current with small variation of generator flux. The dc-bus voltage can be regulated with a master-slave control strategy with cooperation of the LP spool generation subsystem.

B. LP Spool Generation Subsystem and DC-Bus Voltage Regulation

The dc voltage regulation of the proposed hybrid ac/dc generation system is implemented by a master-slave control strategy. The HP generator, while regulating ac load voltage, operates as the master in dc power generation and offers a constant power output to the dc bus. In contrast, the LP generator operates as the slave and supplies the rest of the dc power demand. The dc power output of the LP generator is determined as

$$P_{\rm dc2} = v_{\rm dc} C \frac{dv_{\rm dc}}{dt} + v_{\rm dc} i_{{\rm dc}L} - P_{\rm dc1} \tag{14}$$

where $i_{{\rm dc}L}$ is the dc-bus load current, $P_{\rm dc1}$ and $P_{\rm dc2}$ are the dc power output of the HP and LP generator, respectively.

Other than the dc power extraction from the HP spool generation subsystem, the LP spool generation subsystem operates as a conventional front end dc generation system. The control scheme of the overall generation system will be discussed in greater detail in the next section.

IV. Control Scheme

The overall closed-loop control scheme for the proposed ac/dc hybrid generation system is shown in Fig. 9. The ac load voltage is solely controlled by the HP generator controller. The dc-bus voltage is regulated by a master-slave control strategy, which involves both the HP and LP generator controllers. The dc power output command $P_{\rm dc1}^*$ from HP generator controller (master controller) is designed as a control input commanded by the engine control unit in order to prevent instability issue of the engine caused by high off-take of power extraction on HP spool. An additional control freedom is provided to the engine control unit to balance the power extraction from the HP and LP spools. The operating range of $P_{\rm dc1}^*$ can be calculated and fed back to the engine control unit using (8), (9), and (11). The LP generator controller (slave controller) is commanded to fulfill the rest of the dc power demand from the main dc bus.

Two voltage sensors are used at the ac load terminals of the generator to monitor the ac load voltages. An additional voltage sensor is installed to measure the dc-bus voltage. Four current sensors are used to provide the generator current feedbacks. Neither the rotational speed of rotor nor the rotor position feedback is essential to control the proposed generation system. The control scheme of both the HP and LP spool generation subsystems are discussed in detail in the following sections.

A. Control Scheme for HP Spool Generation Subsystem

The proposed control scheme for HP shaft generation subsystem is shown in Fig. 10. In the HP spool generation subsystem, ac and dc power are generated from the two sides of the HP

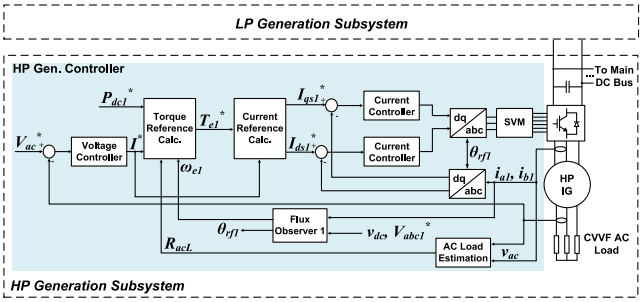

Fig. 10. Proposed closed-loop control scheme for HP spool generation subsystem.

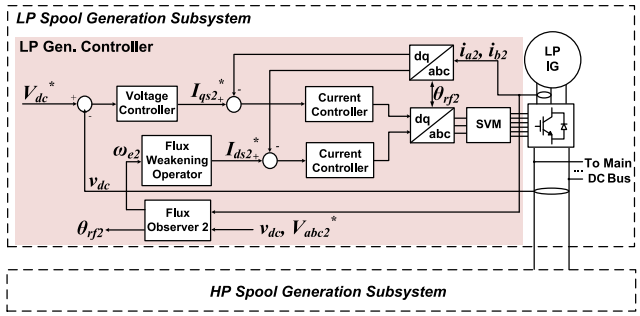

Fig. 11. Closed-loop control scheme for the LP spool generation subsystem.

generator winding, respectively. In order to decouple the ac and dc power supply of the HP spool generation subsystem, the two subsystem control inputs, ac load voltage reference $V_{\rm ac}^*$ and dc output power reference $P_{\rm dc1}^*$, are converted into d- and q-axis current commands of the HP generator. This conversion can be implemented in four steps as follows.

1) Given the reference ac line-to-line RMS load voltage $V_{\rm ac}^*$, a PI controller is used to provide the required ac load current command I^* for regulating the voltage across the three phase balanced resistor (ac loads).
2) The ac load resistance $R_{{\rm ac}L}$ is estimated as the ac load voltage $v_{\rm ac}$ divided by the stator current magnitude I.
3) Given dc power output command $P_{\rm dc1}^*$, ac load current command I^*, ac load resistance $R_{{\rm ac}L}$, and generator electrical frequency ω_{e1}, the torque reference of the HP spool generator T_{e1}^* is calculated using (9).
4) Given the torque reference of the HP spool generator T_{e1}^* and the ac load current command I^*, the d- and q-axis current commands I_{ds1}^* and I_{qs1}^* are obtained from (12) and (13).

The current control loop of the proposed control scheme is based on the field oriented control theory. A direct flux observer from [23] is used to provide the rotor flux speed ω_{e1} and angle θ_{rf1} information. This flux observer inverter requires terminal voltage and generator stator current feedbacks. Since the inverter terminal voltages can be reconstructed using dc-bus voltage feedback and inverter gating signals, only stator current sensor and dc-bus voltage sensor are needed for field orientation. Using rotor flux orientation, two PI controllers are applied in the current control loop to regulate the d-axis current i_{ds1} and q-axis current i_{qs1} of the HP generator. Space vector pulse width modulation (SVPWM) is used to generate gating signals for the active rectifier unit.

B. Control Scheme for LP Spool Generation Subsystem

The closed-loop control scheme for LP shaft generation subsystem is shown in Fig. 11. In the dc-bus voltage control loop, a PI controller is used to generate LP generator q-axis (torque) current command I_{qs2}^*. Since LP shaft generator has a wide speed operating range, flux weakening operation is required in the LP spool generation subsystem. The d-axis (flux) current of the LP generator is commanded to be inversely proportional to the generator shaft speed to obtain a wide speed operation range. The direct flux observer from [23] is used in the LP spool generation subsystem to provide the rotor flux speed ω_{e2} and angle θ_{rf2} information.

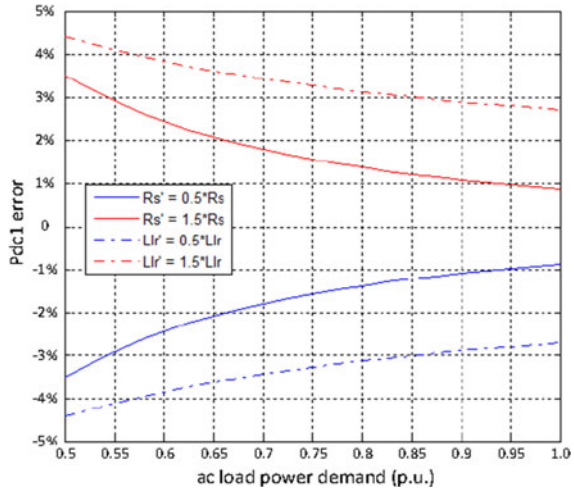

Fig. 12. DC power output error from HP generator stator resistance and rotor leakage inductance estimation inaccuracy.

Similar to the current control loop in HP spool generation subsystem, two PI controllers are applied to regulate d-axis current i_{ds2} and q-axis current i_{qs2} of the LP generator. SVPWM is used to generate gating signals for the active rectifier unit.

C. Robustness Assessment of the Proposed Control Scheme

The overall control scheme robustness toward generator parameter variations greatly depends on the flux orientation in both HP and LP generator controller. The robustness study and parameter sensitivity evaluation of the full-order flux observer [23] used in the proposed control scheme is well documented in [24] and [25].

In the proposed HP spool generation subsystem, the d- and q-axis current reference calculation requires the estimated values of the stator resistance R_{s1}, rotor leakage inductance L_{lr1}, and magnetizing inductance L_{m1} of the HP generator. As a result, the accuracy of the d- and q-axis current reference calculation results can be affected by the discrepancy between the actual and estimated values of the above HP generator parameters.

As is mentioned previously, (12) and (13) are the simultaneous solution of (3) and (8). According to (8), the ac load current reference has no influence with respect to d- and q-axis current reference calculation errors caused by incorrect HP generator

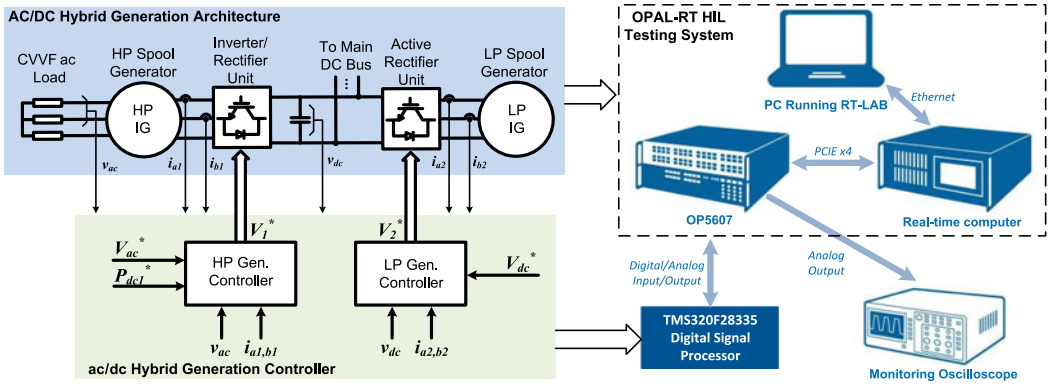

Fig. 13. Hardware-in-the-loop emulation implementation for the proposed ac/dc hybrid generation system.

parameter estimation. Therefore, the robustness of ac load voltage control loop toward the generator parameter variation is superior. However, the inaccurate d- and q-axis current references can result in dc power output error in HP spool generation subsystem.

Among the three generator parameters which have impact to the dc power output regulation precision of the HP spool generation subsystem, the stator resistance R_{s1} and rotor leakage inductance L_{lr1} are relatively small, and contribute minor effect to the regulation robustness degradation. A parameter sensitivity test for dc power output in terms of HP generator stator resistance and rotor leakage inductance is performed using MATLAB. The results of the test are shown in Fig. 12. In this test, the dc power output is commanded to be kept as 1.0 (p.u.), while the ac load power demand varies from 0.5 to 1.0 (p.u.). For $\pm 50\%$ estimation inaccuracy in stator resistance and rotor leakage inductance, the resultant dc power output error is less than 5% throughout the ac load power variation.

The dc power output regulation precision of the HP spool generation subsystem depends greatly on the estimation accuracy of the magnetizing inductance L_{m1} of HP generator. Since the dc-bus voltage regulated in a master-slave strategy, as the master control output, the dc power output error from the HP spool generation subsystem can be compensated by the slave dc voltage controller in LP spool generation subsystem in normal operation. If the HP generator is operated in deep saturation region, saturated magnetizing inductance estimation methods [26]–[28] can be used to improve the dc power output regulation precision of the HP spool generation subsystem.

V. Real-Time Emulation

In order to demonstrate the feasibility of operation of the proposed IG-based ac/dc hybrid generation system, a real-time emulation platform is built using OPAL-RT hardware-in-the-loop (HIL) testing system. The emulated generation system is controlled by a Texas Instrument TMS320F28335 digital signal processor (DSP).

A. Real-Time Emulation Setup

As is shown in Fig. 13, the proposed ac/dc hybrid generation architecture is emulated using the OPAL-RT HIL testing system. The proposed architecture includes the HP generator, the inverter/rectifier unit, and 115-V balanced resistive ac load; as well as the LP generator, the active rectifier unit, and 540-V dc loads on the main dc bus. The OPAL-RT HIL testing platform is consisted of a Virtex 7 FPGA processor and I/O expansion unit (OP5607), a real-time target computer running Redhat operating system (OS), and a PC running the real-time simulation software (RT-LAB). Prior to the real-time emulation, the proposed system model is built and encrypted into FPGA codes in the PC running RT-LAB. The encrypted codes can then be loaded through the target computer running Redhat OS and executed in real time using the OP5607.

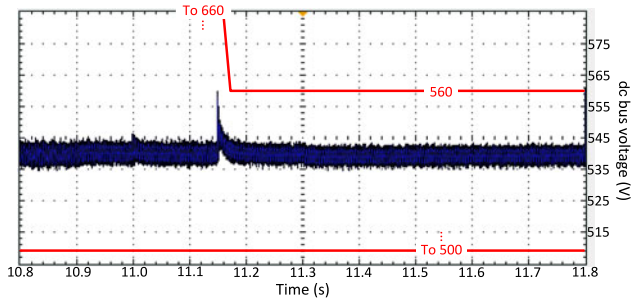

Fig. 14. DC-bus voltage regulation characteristics of the proposed ac/dc hybrid generation system.

The proposed control scheme is implemented in the DSP. The carrier frequencies of the HP and LP generator controllers are set to be 20 and 10 kHz, respectively. The FPGA unit can read the 10 and 20 kHz gating signal through the time-stamped digital input channels of OP5607 and execute the real-time emulation with time steps on nanosecond level. However, the feedback analog signals sent from the OP5607 can only update in every 40 us due to the limited computation power of the target computer. The analog outputs are read by the DSP analog-to-digital converter in every switching period. These feedbacks can also be monitored using an oscilloscope through the same analog output channels.

B. Real-Time Emulation Case Study and Results

A real-time emulation case study is conducted under the HIL platform shown in Fig. 13. In the case study, a 85-kW 11 060-r/min IG and a 60-kW 3150-r/min IG are used on the HP and LP spool, respectively. In the beginning of the emula-

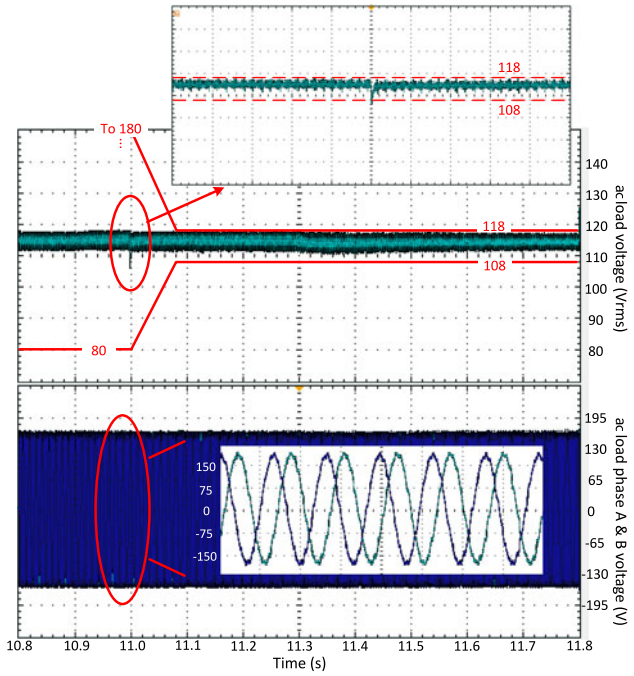

Fig. 15. AC load voltage regulation characteristics of the proposed ac/dc hybrid generation system.

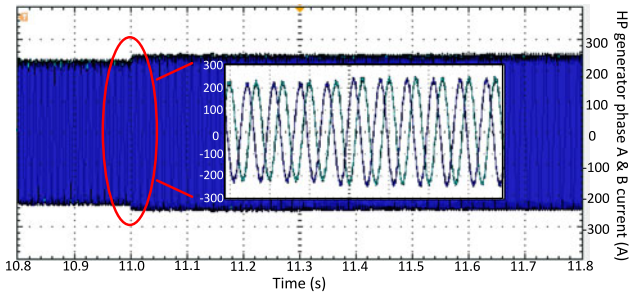

Fig. 16. Phase A and B current characteristics of the HP generator in the proposed ac/dc hybrid generation system.

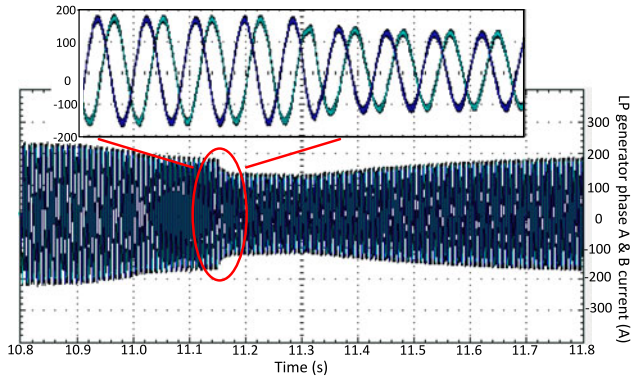

Fig. 17. Phase A and B current characteristics of the LP generator in the proposed ac/dc hybrid generation system.

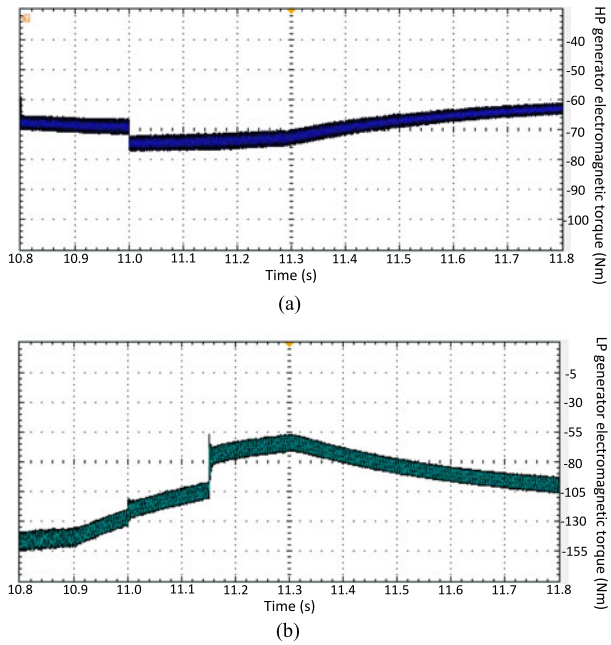

Fig. 18. Electromagnetic torque characteristics of (a) HP and (b) LP generators in the proposed ac/dc hybrid generation system.

tion, the generators are controlled to supply 60-kW three-phase 115-V ac balanced resistive load and 60-kW 540-V dc load at their rated speed. Step changes are applied to the ac load from 60 to 65 kW at 11.0 s, and to the dc load from 60 to 50 kW at 11.15 s. From 10.9 to 11.2 s, the HP and LP generator speed ramp to 110% and 120% of their rated speed, respectively. The dc power output command of the HP spool generation subsystem changes from 20 to 10 kW at 11.3 s.

Currently, airborne electrical power system does not have an official voltage regulation standard for 540-V dc bus. The closest available standard (MIL-STD-704F [29]) is for 270-V dc bus and limits the voltage variation so as not to exceed $+10/-20$ V in steady state. Assuming the voltage variation limitation in MIL-STD-704F is doubled for the 540-V dc bus, the voltage variation allowed for the dc voltage regulation for the proposed system would be $+20/-40$ V. The transient voltage limitation of the proposed system is assumed to be doubled for the same reason.

The dc-bus voltage waveform is shown in Fig. 14, the assumed voltage limit of the 540-V dc bus is illustrated as red lines.

The ac load voltage waveform of the proposed system is shown in Fig. 15, the steady-state and transient voltage limit for a variable frequency 115-V ac distribution in MIL-STD-704F [29] is shown as red lines. The third phase ac voltage is absent because only two voltage sensors are installed to monitor the ac load voltage.

The current waveforms of the HP and LP generators in the proposed system are shown in Figs. 16 and 17. The third phase current is absent because only two current sensors are installed for each generator.

The electromagnetic torque characteristics of the HP and LP generators are illustrated in Fig. 18. When the dc load decreased from 60 to 50 kW at 11.15 s, the HP generator operates as the master and does not react as the dc load changes, while the LP generator decreases its torque to accommodate this load variation. At 11.3 s, the dc power output command changed from

20 to 10 kW. Since the dc power output of the HP spool generation subsystem greatly depends on the flux variation of HP generator, the torque response of HP generator is much slower compared to its immediate reaction to the ac load change at 11.0 s. Clearly, the slow torque response of HP generator is compensated by the fast responded LP generator. Both HP and LP generator respond to the speed variation from 10.9 to 11.2 s. The dc and ac voltage are not affected by the speed variation. The torque characteristics are monitored only for demonstration purposes, no torque transducer is needed for the proposed control scheme.

VI. Conclusion

In this paper, an IG-based ac/dc hybrid generation system for MEA is presented. The application of IG addresses the problem of excessive fault current due to the PM excitation in PM generator-based generation system. The proposed ac/dc hybrid generation architecture supplies CVVF power directly from generator terminals without external exciter. As a result, the hardware requirement is reduced compared to both ac and dc primary generation systems. Both ac and dc output voltages of the system can be well regulated with generator speed, ac and dc side load, and dc power output command variation. The feasibility of operation of the proposed system is demonstrated by HIL real-time emulation.

Appendix

Machine parameters of the HP generator:	
Nominal power (kW)	85
Nominal speed (R/MIN)	11 060
Number of pole pairs	2
Stator resistance (Ω)	0.01373
Rotor resistance (Ω)	0.00931
Stator leakage inductance (mH)	0.049942
Rotor leakage inductance (mH)	0.060791
Magnetizing inductance (mH)	2.9
Primary system parameters of the HP spool generation subsystem:	
Switching frequency (kHz)	20
Current loop controller bandwidth (kHz)	2
Machine parameters of the LP generator:	
Nominal power (kW)	60
Nominal speed (R/MIN)	3150
Number of pole pairs	2
Stator resistance (Ω)	0.0417
Rotor resistance (Ω)	0.0307
Stator leakage inductance (mH)	0.11095
Rotor leakage inductance (mH)	0.084276
Magnetizing inductance (mH)	3
Primary system parameters of the LP spool generation subsystem:	
Switching frequency (kHz)	10
Current loop controller bandwidth (kHz)	1

References

[1] H. Abu-Rub, M. Malinowski, and K. Al-Haddad, *Power Electronics for Renewable Energy Systems, Transportation and Industrial Applications*, Hoboken, NJ, USA: Wiley, 2014.

[2] L. Faleiro, "Summary of the European power optimized aircraft (POA) project," in *Proc. 25th Int. Congr. Aeronautical Sci.*, 2006, pp. 1–4.

[3] B. Bhangu and K. Rajashekara, "Electric starter generators: Their integration into gas turbine engines," *IEEE Ind. Appl. Mag.*, vol. 20, no. 2, pp. 14–22, Mar./Apr. 2014.

[4] K. Muehlbauer and D. Gerling, "Two-generator-concepts for electric power generation in more electric aircraft engine," in *Proc. 19 Int. Conf. Elect. Mach.*, 2010, pp. 1–5.

[5] W. U. N. Fernando, M. Barnes, and O. Marjanovic, "Direct drive permanent magnet generator fed AC-DC active rectification and control for more-electric aircraft engines," *IET Elect. Power Appl.*, vol. 5, no. 1, pp. 14–27, Jan. 2011.

[6] C. R. Avery, S. G. Burrow, and P. H. Mellor, "Electrical generation and distribution for the more electric aircraft," in *Proc. 2007 42nd Int. Univ. Power Eng. Conf.*, Sep. 4–6, 2007, pp. 1007–1012.

[7] M. J. Provost, "The more electric aero-engine: A general overview from an engine manufacturer," in *Proc. 2002. Int. Conf. Power Electron., Mach Drives (Conf. Publ. No. 487)*, 2002, pp. 246–251.

[8] G. A. Whyatt and L. A. Chick, "Electrical generation for more-electric aircraft using solid oxide fuel cells," U.S. Department of Energy, Washington, DC, USA, Contract DE-AC05-76RL01830, 2012.

[9] M. J. Cullen, "Permanent magnet generator options for the more electric aircraft," in *Proc. Int. Conf. Power Electron., Mach Drives (Conf. Publ. No. 487)*, 2002, pp. 241–245

[10] W. Jiabin, K. Atallah, and D. Howe, "Optimal torque control of fault-tolerant permanent magnet brushless machines," *IEEE Trans. Magn.*, vol. 39, no. 5, pp. 2962–2964, Sep. 2003.

[11] G. Jack, B. C. Mecrow, and J. A. Haylock, "A comparative study of permanent magnet and switched reluctance motors for high-performance fault-tolerant applications," *IEEE Trans. Ind. Appl.*, vol. 32, no. 4, pp. 889–895, Jul./Aug. 1996.

[12] C. Mecrow, A. G. Jack, J. A. Haylock, and J. Coles, "Fault-tolerant permanent magnet machine drives," *Inst. Electr. Eng. Proc-Elect. Power Appl.*, vol. 143, pp. 437–442, 1996.

[13] C. Mecrow *et al.*, "Design and testing of a four phase fault-tolerant permanent-magnet machine for an engine fuel pump," *IEEE Trans. Energy Convers.*, vol. 19, no. 4, pp. 671–678, Dec. 2004.

[14] F. Khatounian, E. Monmasson, F. Berthereau, E. Delaleau, and J. P. Louis, "Control of a doubly fed induction generator for aircraft application," in *Proc. 29th Annu. Conf. IEEE Ind. Electron. Soc.*, Nov. 2–6, 2003, vol. 3, pp. 2711–2716

[15] I. Alan and T. A. Lipo, "Starter/generator employing resonant-converter-fed induction machine. I. Analysis," *IEEE Trans. Aerosp. Electron. Syst.*, vol. 36, no. 4, pp. 1309–1328, Oct. 2000.

[16] Y. Jia, U. R. Prasanna, and K. Rajashekara, "An open-end winding induction generation system for frequency insensitive AC loads in more electric aircraft," in *Proc. 40th Annu. Conf. IEEE Ind. Electron. Soc.*, Oct. 29–Nov. 1, 2014, pp. 410–416.

[17] D. W. Novotny and T. A. Lipo, *Vector Control and Dynamics of AC Drives*, Oxford, U.K.: Oxford Univ. Press, 1996.

[18] Y. Jia and K. Rajashekara, "An induction generator based AC/DC hybrid electric power generation system for more electric aircraft," in *Proc. 2015 IEEE Ind. Appl. Soc. Annu. Meeting*, Addison, TX, USA, 2015, pp. 1–7.

[19] R. C. Bansal, "Three-phase self-excited induction generators: an overview," *IEEE Trans. Energy Convers.*, vol. 20, no. 2, pp. 292–299, Jun. 2005.

[20] H. Stemmler and P. Guggenbach, "Configurations of high-power voltage source inverter drives," in *Proc. 1993 5th Eur. Conf. Power Electron. Appl.*, Brighton, U.K., 1993, vol. 5, pp. 7–14.

[21] T. Kawabata, E. C. Ejiogu, Y. Kawabata, and K. Nishiyama, "New open-winding configurations for high-power inverters," in *Proc. IEEE Int. Symp. Ind. Electron.*, Guimaraes, Portugal, 1997, vol. 2, pp. 457–462.

[22] G. Gallegos-Lopez, F. S. Gunawan, and J. E. Walters, "Current control of induction machines in the field-weakened region," *IEEE Trans. Ind. Appl.*, vol. 43, no. 4, pp. 981–989, Jul./Aug. 2007.

[23] C. Lascu, I. Boldea, and F. Blaabjerg, "A modified direct torque control for induction motor sensorless drive," *IEEE Trans. Ind. Appl.*, vol. 36, no. 1, pp. 122–130, Jan./Feb. 2000.

[24] P. L. Jansen, R. D. Lorenz, and D. W. Novotny, "Observer-based direct field orientation: analysis and comparison of alternative methods," in *Proc. Conf. Rec. 1993 IEEE Ind. Appl. Soc. Annu. Meeting*, Toronto, ON, Canada, 1993, vol. 1, pp. 536–543.

[25] P. L. Jansen and R. D. Lorenz, "A physically insightful approach to the design and accuracy assessment of flux observers for field oriented induction machine drives," *IEEE Trans. Ind. Appl.*, vol. 30, no. 1, pp. 101–110, Jan./Feb. 1994.

[26] M. S. Huang and C. M. Liaw, "Improved field-weakening control for IFO induction motor," in *IEEE Trans. Aerosp. Electron. Syst.*, vol. 39, no. 2, pp. 647–659, Apr. 2003.
[27] P. J. Coussens, A. P. Van den Bossche, and J. A. Melkebeek, "Magnetizing current control strategies for nonlinear indirect field oriented control," in *Proc. Conf. Rec. 1995 IEEE Ind. Appl. Conf.*, Orlando, FL, USA, 1995, vol. 1, pp. 538–545
[28] M. Tarbouchi and H. Le Huy, "Control by exact linearization of an induction motor in field weakening regime," in *Proc. 24th Annu. Conf. IEEE Ind. Electron. Soc.*, Aachen, Germany, 1998, vol. 3, pp. 1597–1602
[29] *Department of Defense (United States of America) Interface Standard, Aircraft Electric Power Characteristics*, MIL-STD-704F, Mar. 2004.
[30] G. M. Raimondi *et al.*, "Aircraft embedded generation systems," in *Proc. 2002. Int. Conf. Power Electron., Mach. Drives (Conf. Publ. No. 487)*, Jun. 4–7, 2002, pp. 217–222.
[31] E. Muljadi and T. A. Lipo, "Series compensated PWM inverter with battery supply applied to an isolated induction generator," *IEEE Trans. Ind. Appl.*, vol. 30, no. 4, pp. 1073–1082, Jul./Aug. 1994.
[32] X. Shi and M. Krishnamurthy, "Concept and implementation of a simplified speed control strategy for survivable induction motor drives," in *Proc. IEEE Int. Symp. Ind. Electron.*, Jun. 27–30, 2011, pp. 556–561.
[33] D. Pan, Y. Wang, and T. A. Lipo, "A series regulated open-winding PM generator based constant voltage, variable frequency AC distribution system," in *Proc. 2013 IEEE ECCE Asia Downunder*, Jun. 2013, pp. 214–220.

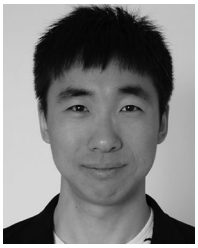

Yijiang Jia (S'13) received the B.S degree in automation from the Beijing University of Technology, Beijing, China, in 2008; the M.S. degree in electrical engineering from the Illinois Institute of Technology, Chicago, IL, USA, in 2012; and the Ph.D. degree in electrical engineering from the University of Texas at Dallas, Richardson, TX, USA, in 2016.

He was an Electronics Mechanical Design Engineer with GE Transportation, Erie, PA, USA from 2012 to 2013. His research interests include electrical power generation system for more electric aircraft and electrical motor drives using wideband gap devices.

Kaushik Rajashekara (F'99) received the Ph.D. degree in electrical engineering from the Indian Institute of Science, Bengaluru, India, 1984.

In 1989, he joined the Division of General Motors Corporation, Delphi, Indianapolis, IN, USA, as a Staff Project Engineer. In Delphi and General Motors, he held various lead technical and managerial positions, and was a Technical Fellow and the Chief Scientist for developing electric machines, controllers, and power electronics systems for electric, hybrid, and fuel cell vehicle systems. In 2006, he joined Rolls-Royce Corporation, Indianapolis, IN, USA as a Chief Technologist for more electric architectures and power conversion/control technologies for aero, marine, defense, and energy applications. In August 2012, he joined as a Distinguished Professor of engineering the University of Texas at Dallas, Dallas, TX, USA. Since September 2016, he has been a Distinguished Professor with the University of Houston, Houston, TX. He has published more than 150 papers in international journals and conferences, and has more than 45 patents. He has co-authored one IEEE Press book on sensorless control of ac motor drives. His research interests include the area of power electronics, drives, and energy management of microgrid systems.

Dr. Rajashekara was elected as a member of the National Academy of Engineering in 2012 for contributions to electric power conversion systems in transportation. He was also elected as a fellow of the National Academy of Inventors and of the Indian National Academy of Engineering. He received the IEEE Richard Harold Kaufmann Award, the IEEE Industry Applications Society (IAS) Outstanding Achievement Award, and the IEEE IAS Gerald Kliman Award for contributions to the advancement of power conversion technologies through innovations and their applications to industry. He is a fellow of Society of Automotive Engineers (SAE) International.